Serine as environmentally friend corrosion inhibitor for low chromium steel T22 in sulfamic acid solutions

Sayed S. Abd El Rehim[1], Hesham T.M. Abdel-Fatah[2],* Hala E.E. El-Sehiety[2]

[1] Chemistry Department, Faculty of Science, Ain Shams University, Abbassia, Cairo, EGYPT.

[2] Central Chemical Laboratories, Egyptian Electricity Holding Company, Sabtia, Cairo, EGYPT.

* E-mail: hesham_tm@yahoo.com

Abstract

The performance of Serine as a non-toxic corrosion inhibitor for low chromium alloy steel in 0.5M Sulfamic acid solutions have been investigated by various electrochemical techniques. The study was performed using Linear Polarization Resistance (LPR) and Electrochemical Impedance Spectroscopy (EIS) as well as the recent technique Electrochemical Frequency Modulation (EFM). The results of the investigation show that the inhibition efficiency increased with increasing inhibitor concentration, but decreased with increasing the solution temperature and stirring velocity. All the collected results from the three techniques are in good agreements, which confirm the ability of EFM technique for monitoring the corrosion inhibition under the studied conditions.

Keywords: corrosion inhibition, acid solutions, amino acids, sulfamic acid, LPR, EIS, EFM.

1- Introduction

Sulfamic acid (HSO_3NH_2) is widely used in various industrial acid cleaning

applications.

However, little work has been reported on the corrosion behavior of different metal

materials in sulfamic acid solutions. Sulfamic acid has many advantages such as [1-3]:

- It is strong acid in aqueous solution with remarkable effectiveness for dissolving

   iron oxides and variety of water- formed scales.

- It is compatible with alloy steels and austenitic stainless steels.

- It is crystalline solid, highly stable, odorless and easily to store and handle.

- It has negligible effect on the skin.

Low chromium steels are widely used for manufacturing different sections of steam

power plants [4,5].

Because of the aggressiveness of acid solutions, corrosion inhibitors are one of the most

effective and economic corrosion control methods to protect metal corrosion in acidic media

[6,7]. The uses of corrosion inhibitors in specific applications such as the acid cleaning

of steam generators are shortly reviewed [8].

Most of the investigations on corrosion inhibitors in acid media have been made in

static conditions. Only few studies in the literatures discuss the effect of solution

movement (hydrodynamic condition) on the inhibition efficiency [9,10].

Increasing awareness of health and ecological risks has drawn attention to use of

substitute non-toxic compounds [11,12].

The properties of amino acids would justify their use as non-toxic corrosion inhibitors

for iron, steel and stainless steel [12-16].

The purpose of the present study is to investigate the effectiveness of one amino acid Serine (HOCH$_2$CHCOOH) as a non-toxic corrosion inhibitor for low chromium steel (LCrS) in 0.5M sulfamic acid solutions and to evaluate the effect of inhibitor concentrations, solution temperature and solution stirring on the corrosion inhibition efficiency.

2- Experimental

The experiments were performed on low chromium steel (ASTM A213 grade T22) strips. Table (1) presents the chemical composition (wt.%) of the used alloy. The electrochemical experiments were carried out using a three-electrode glass cell assembly of 150 cm^3 volume capacity. The cell consists of a low chromium steel (LCrS) electrode embedded in epoxy resins with an exposed area of (1cm^2) as a working electrode, a saturated calomel electrode as a reference electrode, and a platinum foil (1cm^2) as a counter electrode. The working electrodes were polished mechanically with fine grade emery papers, degreased with acetone in an ultrasonic bath, washed with doubly distilled water and finally dried before use.

All solutions were freshly prepared from analytical grade chemical reagents using doubly distilled water. The experiments were conducted in stagnant aerated solutions at different temperatures 25, 35, 45 and 55 ^{o}C ±2. Some experiments were carried out at different stirring velocities (200, 400, 800 and 1200 RPM) using adjustable digital magnetic stirring hotplate DAIHAN, Model MSH 20.

The Electrochemical Frequency Modulation (EFM) technique is a new tool for monitoring the electrochemical corrosion. The theory of EFM technique is reported before [17]. The Intermodulation spectra contain current responses assigned for harmonical and intermodulation current peaks. The higher peaks were used to directly

determines the values of the corrosion current density (I_{corr}), corrosion rate, the Tafel constants (β_c and β_a) and the causality factors (CF2 & CF3). Electrochemical Frequency Modulation technique has many features such as **[17-19]**:

- It is considered to be a non-destructive technique.

- It has an internal self-check in the form of the two "Causality Factors". These two factors should have the values 2.0 and 3.0 if all of the conditions of EFM theory have been met.

- It is a fast test (requires only few minutes).

Impedance spectra were recorded at open circuit potentials in the frequency range between 15 kHz and 300 mHz. While the EFM measurements were performed with applying potential perturbation signal with amplitude of 10 mV with two sine waves of 2 and 5 Hz.

For Linear Polarization Resistance (LPR) measurements, a sweep from −20 to +20 mV versus open circuit potential at a sweep rate of 5 mV s^{-1} was used and the polarization resistance (R_p) was measured from the slope of potential versus current curve in the vicinity of corrosion potential.

All Electrochemical experiments were carried out using Gamry PCI300/4 Potentiostat/Galvanostat/Zra analyzer, DC105 Corrosion software, EIS300 Electrochemical Impedance Spectroscopy software, EFM140 Electrochemical Frequency Modulation software and Echem Analyst 5.21 for results plotting, graphing, data fitting and calculating.

3- Results and Discussion

3-1 Effect of inhibitor concentration and temperature

The inhibition efficiency of Serine (Ser) for LCrS in aerated 0.5M sulfamic acid solution was determined at different temperatures 25, 35, 45 and 55 ^{o}C ±2 by using three different electrochemical techniques as following:

3-1-1 Electrochemical Frequency Modulation studies:

Figures (1a and 1b) are examples demonstrate the EFM intermodulation spectra of LCrS in aerated stagnant 0.5M sulfamic acid in absence and presence of 0.06M Ser at 55°C. Similar results were collected for the other Ser concentrations at different temperatures.

The values of kinetic parameters such as I_{corr}, β_a, β_c, and the both Causality Factors (CF2 and CF3) for Ser are given in Table (2). Inspections of these data infer the following:

- The addition of Ser to 0.5M sulfamic acid solution decreases the corrosion current density (I_{corr}) indicating that Ser acts as corrosion inhibitor.

- With increasing the inhibitor concentration the corrosion current density (I_{corr}) decreases as a result of increasing adsorption and surface coverage of Ser on the steel surface.

- The corrosion current density (I_{corr}) in the absence and presence of Ser increases with increasing the temperature indicating that the corrosion rate increases with temperature in both inhibited and uninhibited solutions. Moreover, it is seen that the values of (I_{corr}) are higher in the uninhibited sulfamic acid solution than those obtained in the inhibited solution indicating the inhibitive effect of Ser at all tested temperature.

The inhibition efficiency (IE%) of Serine was calculated using the following equation:

$$IE\% = \left[1 - \left(\frac{I_{corr}}{I^{o}_{corr}}\right)\right] \times 100 \qquad (1)$$

where I^{o}_{corr} and I_{corr} are the corrosion current densities for uninhibited and inhibited solutions, respectively.

The calculated values of the inhibition efficiency (IE%) in different concentrations of Ser (0.01M to 0.06M) and at different temperatures (25 ^{o}C - 55 ^{o}C) are also included in Table (2). The values of IE% show that the corrosion process depends on the both factors, the inhibitor concentration and the solution temperature.

At a given temperature, the IE% increases with the increasing Ser concentration as a result of increasing adsorption and surface coverage on the electrode surface. However, at a given Ser concentration, the IE% decreases with the increase of solution temperature. Such behaviour may be conducted with two effects [20]; a certain drawing of adsorption-desorption equilibrium towards desorption and roughening of the metal from enhanced corrosion.

3-1-2 Electrochemical Impedance studies:

Typical Nyquist plots (representative example) obtained for LCrS electrode in aerated stagnant 0.5M sulfamic acid solution free and containing different concentrations of Ser at 45 ^{o}C at OCP are shown in Figure (2). Similar impedance plots of LCrS at different temperatures were obtained (diagrams not given). In all these cases the plots have the same shape where a single depressed capacitive semicircle was obtained. This frequency dispersion can be attributed to inhomogeneties and roughness of the electrode surface [21,22]. The presence of one semicircle indicates that only one reaction

controlling the corrosion process. This reaction is a general corrosion of the surface in contact with the solution.

Table (3) shows the impedance parameters, the double layer capacitance, C_{dl} and the charge transfer resistance, R_{ct} (the diameter of the capacitive loop). Revisions of the collected data listed in this table indicates the following:

- The charge transfer resistance (R_{ct}) increases and the double layer capacitance (C_{dl}) decreases as the inhibitor concentration is increased. The increase in charge transfer resistance may be the result of decreasing film capacitance due to increase the surface coverage by the inhibitor molecules.

- The values of (R_{ct}) decrease and those of (C_{dl}) increase with increasing temperature.

The above results can be explained on the basis that adsorption of the inhibitor species and formation of a physical protective film that retard the charge transfer process and therefore increases the value of (R_{ct}) and so the corrosion reactions were inhibited. Moreover, the adsorbed inhibitor species decrease the electrical capacity of the electrical double layer at the electrode/solution interface and therefore decrease the values of (C_{dl}) [23].

Since the electrochemical theory assumes that the reciprocal of charge-transfer resistance ($1/R_{ct}$) is directly proportional to the corrosion rate. The inhibition efficiency (IE%) was calculated from (R_{ct}) values using the following Equation:

$$ IE\% = \left[1 - \left(\frac{R^{o}_{ct}}{R_{ct}} \right) \right] \times 100 \qquad (2) $$

where R^{o}_{ct} and R_{ct} are the charge-transfer resistance values in the absence and presence of inhibitor, respectively.

The calculated values of the inhibition efficiency (IE%) for different concentrations of

Ser at different temperatures are also included in Table (3). The values of IE% show

that the corrosion process depends on the both factors, the inhibitor concentration and

the solution temperature. The IE% increases with the increase of the inhibitor

concentration, but it decreases with the increase of solution temperature.

3-1-3 Linear Polarization Resistance measurements:

The effect of addition of various concentrations of Ser on the corrosion behavior of

LCrS in 0.5M sulfamic acid solution was investigated by potentiodynamic polarization

technique. Figure (3) displays as an example of the cathodic and anodic polarization

curves of LCrS in 0.5M sulfamic acid solution devoid of and containing various

concentrations of Ser at 55 ^{o}C. Similar polarization curves for other temperatures were

obtained (diagrams not given).

The values of the polarization resistance (R_p), and the inhibition efficiency (IE%) for

different concentrations of Ser at different temperatures are included in Table (3). The

inhibition efficiency (IE%) of Ser was calculated using Equation (3).

$$IE\% = \left[1 - \left(\frac{R^{o}_{p}}{R_{p}} \right) \right] \times 100 \qquad \textbf{(3)}$$

where R^{o}_{p} and R_p are the polarization resistance values in the absence and presence of

inhibitor, respectively.

The IE% value increases by an increase in Ser concentration and decreases with the

rise of temperature.

3-1-4 Apparent activation energy:

Further study of the effect of temperature on the inhibition efficiency was carried out.

Corrosion activation energies (E_a) in absence and presence of the inhibitor were

calculated using the following Arrhenius equation:

$$\log (\text{Corr. Rate}) = \frac{-E_a}{2.303RT} + A \qquad (4)$$

where E_a is the apparent activation energy, R is the universal gas constant, T is the

absolute temperature, and A is the Arrhenius pre-exponential factor.

A plot of logarithm of the corrosion rate of LCrS obtained from the three techniques

versus 1/T gives straight lines their slopes are the $-E_a$/2R. Figure (4) is an example of

Arrhenius curves obtained from LPR technique.

In the literature, the lower activation energy value of corrosion process in the presence of

inhibitor rather than the absence of inhibitor is attributed to its chemisorption, while it

is found to be opposite in the case with physical adsorption **[24-26]**.

The calculated values of E_a extracted from the three techniques were given in Table (4).

The analysis of E_a values shows that an increasing in corrosion activation energy in the

presence of inhibitor compared to its absence with a decrease in inhibition efficiency

with the rise in temperature indicates that the type of adsorption of Ser on the steel

surface in 0.5M sulfamic acid solutions belongs to physical adsorption.

3-2 Effect of solution stirring on the inhibition efficiency:

The corrosion inhibition of Ser for LCrS in aerated stirring 0.5M sulfamic acid solutions at

stirring speeds (RPM) 200, 400, 800 and 1200 and at 25 ^{o}C were carried out using

EFM and EIS techniques. The EFM and EIS diagrams for LCrS in aerated stirring

0.5M sulfamic acid in absence and presence of 0.06M Ser at different stirring velocities were collected. Figure (5) is an example that represents the EFM intermodulation spectra of LCrS in aerated stirring 0.5M sulphamic acid containing 0.06M Ser at 800 RPM.

The obtained results from EFM and EIS techniques were presented in Table (5). This table demonstrates the effect of stirring speed on the inhibition efficiency of 0.06M Ser. Inspections of the produced results of the both techniques reveal the following:

- The results obtained from the EIS and EFM support that the inhibiting effect of Ser is strongly dependent on the solution movement (hydrodynamic conditions). As the stirring velocity increases, the efficiency of the inhibitor decreases.

- At 0.06M of Ser concentration, the corrosion current density (I_{corr}) increases while (R_{ct}) decreases with increasing the stirring speed as a result of removal of adsorbed inhibitor species from the metal surface which retards the effectiveness of the inhibitor and thus significantly enhances the corrosion rate [3,27,28].

- The corrosion inhibition efficiency under stagnant conditions is higher than that of the inhibition performance under stirring conditions.

3-3 Adsorption Isotherms

Adsorption isotherm was studied in order to get more information about the interaction between the adsorbed organic inhibitor species and the metal surface and therefore, the mechanism of corrosion inhibition [26,27].

Two main types of interactions can classify the adsorption of organic compounds: physical adsorption (physisorption) and chemical adsorption (chemisorption). They are influenced by the nature of the charge of the metal surface, the chemical structure of the inhibitor and the type of electrolyte.

Surface coverage degree (θ) is important parameter for determining the inhibitor adsorption characteristics. The surface coverage degree (θ), as a function of inhibitor concentration was calculated (θ = IE% / 100). Surface coverage values for different concentrations of Ser in 0.5M sulfamic acid solution at different temperatures are given in Tables (2 and 3) using the obtained data from the three techniques.

The surface coverage (θ) results were fitted to different isotherm type models to represent the adsorption behavior of Ser on the steel surface. The best-fitted straight line was obtained for the plot of the surface coverage (θ) versus logarithm of inhibitor concentration (C_{inh}). This suggests that the adsorption of Ser at the steel surface in sulfamic acid solutions have been found to obey the Temkin adsorption isotherm [28,29].

Figure (6) is an example of Temkin adsorption isotherm for various concentrations of Ser at different temperatures using the data obtained from EFM measurements.

The equilibrium constant (K_{ads}) was calculated from the intercepts and slopes of the straight lines of Temkin isotherm curves.

The equilibrium constant of adsorption (K_{ads}) is related to the standard free energy of adsorption, (ΔG^{o}_{ads}) via the following Equation (5):

$$K_{ads} = \frac{1}{55.5} \exp\left(\frac{-\Delta G^{o}_{ads}}{RT}\right) \qquad (5)$$

where R is the universal gas constant and T is the absolute temperature. The value of (55.5) is the concentration of water in the solution in (mol l^{-1}) [30,31].

The equilibrium constant (K_{ads}) and the standard free energy of adsorption, (ΔG^{o}_{ads}) values obtained from the data of the three techniques are listed in Table (6).

As shown in Table (6), the values of (K_{ads}) decrease with increasing the temperature, which confirming the suggestion that Ser is physically adsorbed on the surface of LCrS [32-34].

The values of the standard free energy of adsorption , (ΔG^{o}_{ads}) acquire a negative sign emphasis the spontaneity of the adsorption process and stability of the adsorbed layer on the LCrS surface which accompanied with a high efficient adsorption of Ser [35].

It was reported before that the values of ($\Delta G^{o}_{ads} < 40$ kJ mol^{-1}) as an indicator of physical adsorption (electrostatic interactions between the inhibitor species and the charged metal surface). While values of ($\Delta G^{o}_{ads} \geq 40$ kJ mol^{-1}) are related to chemical adsorption (sharing or transfer of electrons from organic molecules to the metal surface to form a coordinate bond [36-41]. Therefor, the calculated values of (ΔG^{o}_{ads}) listed in Table (6) indicating that the adsorption mechanism of Ser at LCrS surface in 0.5M sulfamic acid solutions is typical of physisorption.

3-4 Inhibition Mechanism

All the above results emphasis that the Ser acts as inhibitor for LCrS in 0.5M sulfamic acid solutions.

The corrosion inhibition of Ser is due to their physical adsorption and formation of protective film on the steel surface.

The pervious investigation reports that the steel surface in aqueous acid solutions is positively charged [42-44]. Moreover, in aqueous acid solutions, the amino acids exist either as neutral molecules or in the form of cations (protonated) [19,45,46]. Therefore, these amino acids may be adsorbed on the positively charged metal surface in the form

of neutral molecules involving the displacement of water molecules from the metal surface and sharing electrons between the nitrogen atoms and the metal surface [47]. Furthermore, adsorption can occur via the already adsorbed sulfamate anions at the positively charged metal surface. The adsorbed sulfamate anions at the metal surface make a negatively charged double layer and consequently it results in an increase in the adsorption capability of the protonated amino acids [44,48].

Conclusion

The addition of small amounts of Ser to the 0.5M sulfamic acid solution inhibits the corrosion of low chromium alloy steel. Ser acts as effective inhibitor and the corrosion inhibition efficiency of about 84% was recorded. The mechanism of the corrosion inhibition process is based on the adsorption of Ser on the active corrosion sites of the alloy surface. The Adsorption of Ser molecules onto the steel surface follows the Temkin's adsorption isotherm. The inhibition efficiency is clearly depends on the inhibitor concentration, the solution temperature and the solution stirring velocity. The inhibition efficiency increases with the increase of inhibitor concentration but decreases with the increase of solution temperature and solution stirring. The collected data from the three methods at different experimental conditions are in good agreements and similar trend, which confirm that the EFM technique can be relied upon for monitoring the corrosion inhibition under the studied conditions.

References:

1- M. D. Majnouni, Arif E. Jaffer, International Water Conference, paper no. IWC-03-34, Pittsburgh, 2003.

2- Jemes W. McCoy, Industrial chemical cleaning, Chemical Publishing Co., ISBN 0-8206-0305-8, New York, USA 1984.

3- M. S. Morad, J Appl. Electrochem., 38 (11) (2008) 1509.

4- G.M.W. Mann, High Temperature High Pressure Electrochemistry in Aqueous Solutions, NACE-4, Houston, USA, 1976, p34.

5- W.A. Ghanem, F.M. Bayyoumi, B.G. Ateya, Corros. Sci., 38 (1996) 1171.

6- A. U. Malik, M. F. Al Ghamdi, A. H. Hodhan, 9th Middle East Corros. Conf. and Exhibition, 2001: p. 457.

7- Sayed S. Abdel Rehim, Omar A. Hazzazi, Mohammed A. Amin, Khaled F. Khaled, Corros. Sci., 50 (2008) 2258.

8- R. Gabriele, Corrosion Reviews. 20 (6) (2002) 509.

9- H. Ashassi-Sorkhabi, E. Asghari, Electrochim. Acta, 54 (2008) 162.

10- X. Jiang, Y.G. Zheng, W. Ke, Corros. Sci., 47 (2005) 2636.

11- M. Lebrini, M. Traisnel, M. Lagrenee B. Mernari, F.Bentiss, Corros. Sci., 50 (2008) 473.

12- E.E. Oguzie, Y. Li, F.H. Wang, J. Colloid Interface Sci., 310 (2007), 90.

13- H. Ashassi-Sorkhabi, Z. Ghasemi, D. Seifzadah, Appl. Surf. Sci., 249 (2005) 408.

14- D. J. Kalota, D.e. Silverman, Corrosion, 50 (1994) 138.

15- L. Madkour, M. Ghoneim, Bull. Electrochem., 13 (1997) 1.

16- M.S.S. Morad, A.E-H.A. Hermas, M.A.S. Aal, J. Chem. Technol. Biotechnol., 77 (2002) 486.

17- R.W.Bosch, J.Hubrecht, W.F.Bogaerts, B.C.Syrett, Corrosion, 57 (2001), 60.

18- S.S.Abdel-Rehim, K.F.Khaled, N.S.Abd-Elshafi, Electrochim. Acta, 51 (2006) 3269.

19- Mohammed A. Amin, Sayed S. Abd El Rehim, Hesham T.M. Abdel-Fatah, Corros. Sci. 51 (2009) 882.

20- M.A.Amin, S.S.Abd EI-Rehim, E.E.F.El-Sherbini , R.S.Bayoumi, Int. J. Electrochem. Sci., 3 (2008) 199.

21- T. Paskossy, J. Electroanal. Chem., 364 (1994) 111.

22- F.B. Growcock, J.H. Jasinski, J. Electrochem. Soc., 136 (1989) 2310.

23- F. Mansfield, Corrosion Mechanism, Marcel Dekker, New York (1987) 119.

24- J.L. Mora-Mendoza, S. Turgoose, Corrosion 2001, NACE, USA, Paper 63, 2001.

25- V. Jovancicevic, S. Ramachandran, P. Prince, Corrosion, 55 (5) (1999) 449.

26- S. T. Hirozawa, Proc. 8th Eur. Symp. Corros. Inhib. Ann. University, Ferrara, Italy, 1 (1995) 25.

27- M. Lebrini, M. Lagrenée, H. Vezin, M. Traisnel, F. Bentiss, Corros. Sci., 49 (2007) 2254.

28- E.E. Oguzie, C. Unaegbu, C.N. Ogukwe, B.N. Okolue, A.I. Onuchukwu, Mater. Chem. Phys., 84 (2004) 363.

29- D. Do Duong, "Adsorption Analysis: Equilibria and Kinetics", Imperial College Press, London, UK, 1980, pp. 10.

30- A. Yurt, A. Balaban, S.U. Kandemir, G. Bereket, B. Erk, Mater. Chem. Phys., 85 (2004) 420.

31- L. Larabi, O. Benali, S.M. Mekelleche, Y. Harek Appl. Surf. Sci., 253 (2006) 1371.

32- S.T.Keera, M.A.Deyab, Colloids and Surfaces A: Physicochem. Eng. Aspects 266 (2005) 129.

33- S.S.Abd El Rehim, H.H.Hassan, M.A.Amin, Mater. Chem. Phys., 78 (2002) 337.

34- M. El Azhar, M. Traisnel, B. Mernari, L. Gengembre, F. Bentiss, M. Lagrenee, Appl. Surf. Sci., 185 (2002) 197.

35- A.Y. El-Etre, Appl. Surf. Sci., 252 (2006) 8521.

36- H.Ashaasi-Sorkhabi, M.R. Majidi, K. Seyyedi, Appl. Surf. Sci., 225 (2004) 176.

37- F.M. Donahue, K. Nobe, J. Electrochem. Soc., 112 (1965) 886.

38- E. Khamis, F. Bellucci, R.M. Latanision, E.S.H. El-Ashry, Corrosion, 47 (1991) 677.

39- M. Bouklah, A. Attayibat, S. Kertit, A. Ramdani, B. Hammouti, Appl. Surf. Sci., 242 (2005) 399.

40- M. Scendo, Corros. Sci. 49 (2007) 373.

41- M. Bouklah, B. Hammouti, M. Lagrene´e, F. Bentiss, Corros. Sci., 48 (2006) 2831.

42- M. Lagrenee, B. Mernari, M. Bouanis, M. Traisnel, F.Bentiss, Corros. Sci., 44 (2002) 573.

43- R. Solmaz, G. Kardas, B. Yazc , M. Erbil, Colloids Surf. A Physicochem. Eng. Aspects 312 (2008) 7.

44- M. H. Wahdan, A. A. Hermas and M. S. Morad, Mater. Chem. Phys., 76 (2002) 111.

45- J. O'M. Bockris and B. Yang, J. Electrochem. Soc., 138 (1991) 2237.

46- M. Abdallah and H. E. Megahed, Monatshefte für Chemie, 126, 519 (1995).

47- F. Bentiss, M. Traisnel, L. Gengembre, M. Lagrenee, Appl. Surf. Sci., 152 (1999) 237.

48- L. Larabi, Y. Harek, M. Traisnel, and A. Mansri, J. Appl. Electrochem., 34 (2004) 833.

Table (1): Chemical composition (wt.%) of LCrS

Alloy	Si	Mn	Cr	Fe	Mo
ASTM A213 grade T22	0.37	0.68	2.41	95.62	0.92

Table (2): Electrochemical kinetic parameters obtained from EFM technique for LCrS in 0.5M sulfamic acid with various concentrations of Ser at different temperatures

Temp (°C)	Ser Conc (M)	β_a (mV.dec^{-1})	β_c (mV.dec^{-1})	CF2	CF3	I_{corr} (µA.cm^{-2})	IE%	θ
25	0.00	58.28	181.74	1.878	3.336	565.07	0.00	0.000
	0.01	57.88	179.54	1.911	2.836	376.72	33.33	0.333
	0.02	56.51	177.82	1.838	2.998	289.49	48.77	0.488
	0.04	56.23	176.92	2.017	3.067	169.95	69.92	0.699
	0.06	54.53	174.78	1.968	2.889	89.11	84.23	0.842
35	0.00	78.79	201.64	1.845	3.203	837.15	0.00	0.000
	0.01	78.62	201.44	1.949	2.925	688.77	17.72	0.177
	0.02	78.43	199.93	2.091	3.091	583.36	30.32	0.303
	0.04	77.72	198.56	1.832	3.014	372.68	55.48	0.555
	0.06	76.69	198.41	1.807	2.551	213.60	74.49	0.745
45	0.00	89.24	203.87	2.003	2.835	1263.98	0.00	0.000
	0.01	88.52	199.72	2.021	2.784	1184.73	6.27	0.063
	0.02	87.91	198.68	1.987	2.997	933.11	26.18	0.262
	0.04	86.53	197.85	2.011	3.067	635.24	49.74	0.497
	0.06	86.92	196.18	1.965	3.104	397.36	68.56	0.686
55	0.00	86.78	199.45	1.857	3.342	1927.57	0.00	0.000
	0.01	85.92	196.78	1.964	2.911	1691.79	12.23	0.122
	0.02	85.81	196.54	2.073	2.846	1378.12	28.50	0.285
	0.04	86.91	197.04	1.867	2.577	1092.50	43.32	0.433
	0.06	86.27	198.51	2.046	3.054	672.64	65.10	0.651

Table (3): Electrochemical kinetic parameters obtained from EIS and LPR techniques for LCrS in 0.5M sulfamic acid with various concentrations of Ser at different temperatures

Temp (°C)	Ser Conc (M)	EIS				LPR		
		C_{dl} (μF.cm^{-2})	R_{ct} (ohm.cm^2)	IE%	θ	R_p (ohm.cm^2)	IE%	θ
25	0.00	826.7	33.63	0.00	0.000	33.78	0.00	0.000
	0.01	565.8	49.89	32.59	0.326	49.44	31.67	0.317
	0.02	437.7	64.54	47.89	0.479	63.26	46.60	0.466
	0.04	269.9	107.22	68.63	0.686	106.68	68.34	0.683
	0.06	138.2	204.13	83.53	0.835	198.67	83.00	0.830
35	0.00	874.1	23.01	0.00	0.000	24.39	0.00	0.000
	0.01	611.3	35.71	35.56	0.356	35.81	31.89	0.319
	0.02	511.5	42.12	45.37	0.454	41.87	41.75	0.417
	0.04	331.2	64.89	64.54	0.645	64.64	62.27	0.623
	0.06	199.6	113.66	79.76	0.798	111.97	78.22	0.782
45	0.00	967.8	17.44	0.00	0.000	18.38	0.00	0.000
	0.01	728.8	24.62	29.16	0.292	22.57	18.56	0.186
	0.02	644.9	28.29	38.35	0.384	28.21	34.85	0.348
	0.04	452.8	40.96	57.42	0.574	40.86	55.02	0.550
	0.06	266.6	66.26	73.68	0.737	66.08	72.19	0.722
55	0.00	1113.7	13.00	0.00	0.000	12.98	0.00	0.000
	0.01	929.9	15.36	15.36	0.154	15.39	15.66	0.157
	0.02	768.9	18.80	30.85	0.309	18.78	30.88	0.309
	0.04	591.3	24.86	47.71	0.477	24.06	46.05	0.461
	0.06	382.4	39.08	66.73	0.667	39.00	66.72	0.667

Table (4): Activation energies of Ser using the obtained data from the three techniques

Ser Conc (M)	E_a (kJ mol^{-1})		
	EFM	EIS	LPR
0.00	34.57	34.28	34.45
0.01	41.23	40.13	40.64
0.02	42.16	42.33	41.83
0.04	49.93	48.68	49.31
0.06	54.65	54.71	53.99

Table (5): Effect of stirring speed (RPM) on the inhibition efficiency of Ser using the obtained data from EFM and EIS techniques

Compound	200 RPM		400 RPM		800 RPM		1200 RPM	
	I_{corr} (µA.cm^{-2})	R_{ct} (ohm.cm^2)	I_{corr} (µA.cm^{-2})	R_{ct} (ohm.cm^2)	I_{corr} (µA.cm^{-2})	R_{ct} (ohm.cm^2)	I_{corr} (µA.cm^{-2})	R_{ct} (ohm.cm^2)
Blank	637.57	31.25	829.77	27.12	1239.15	23.85	1915.37	18.37
0.06M Ser	127.95	147.67	191.24	111.31	344.26	84.56	665.39	51.28
IE%	79.93	78.84	76.95	75.64	72.22	71.80	65.26	64.18

Table (6): The calculated equilibrium constant and standard free energy of adsorption for Ser using the obtained data from the three techniques

Technique	25 °C		35 °C		45 °C		55 °C	
	K_{ads}	$\Delta G^{o}{}_{ads}$ (kJ mol^{-1})	K_{ads}	$\Delta G^{o}{}_{ads}$ (kJ mol^{-1})	K_{ads}	$\Delta G^{o}{}_{ads}$ (kJ mol^{-1})	K_{ads}	$\Delta G^{o}{}_{ads}$ (kJ mol^{-1})
EFM	303.84	-24.11	272.04	-24.64	218.78	-24.86	174.20	-25.02
EIS	302.89	-24.11	271.09	-24.63	217.83	-24.85	170.07	-24.96
LPR	297.38	-24.06	274.09	-24.66	219.35	-24.87	172.93	-25.00

Figures Captions

Figure (1):   (a) Intermodulation Spectrum for LCrS in 0.5M sulfamic at 55 ^{o}C

(b) Intermodulation Spectrum for LCrS in 0.5M sulfamic in presence

of 0.06M Serine at 55 ^{o}C

Figure (2):   Nyquist plots for LCrS in 0.5M sulfamic without and with various

concentrations of Serine at 45 ^{o}C

Figure (3):   Polarization curve for LCrS in 0.5M sulfamic without and with

various concentrations of Serine at 55 ^{o}C

Figure (4):   Arrhenius plots for LCrS in 0.5M sulfamic without and with various

concentrations of Serine associated with LPR measurements

Figure (5):   Intermodulation Spectrum for LCrS in 0.5M sulfamic in presence of

0.06M Serine at 800RPM

Figure (6):   Temkin isotherm plots for LCrS in 0.5M sulfamic in presence of

various concentration of Serine at different temperatures (data

obtained from EFM technique)
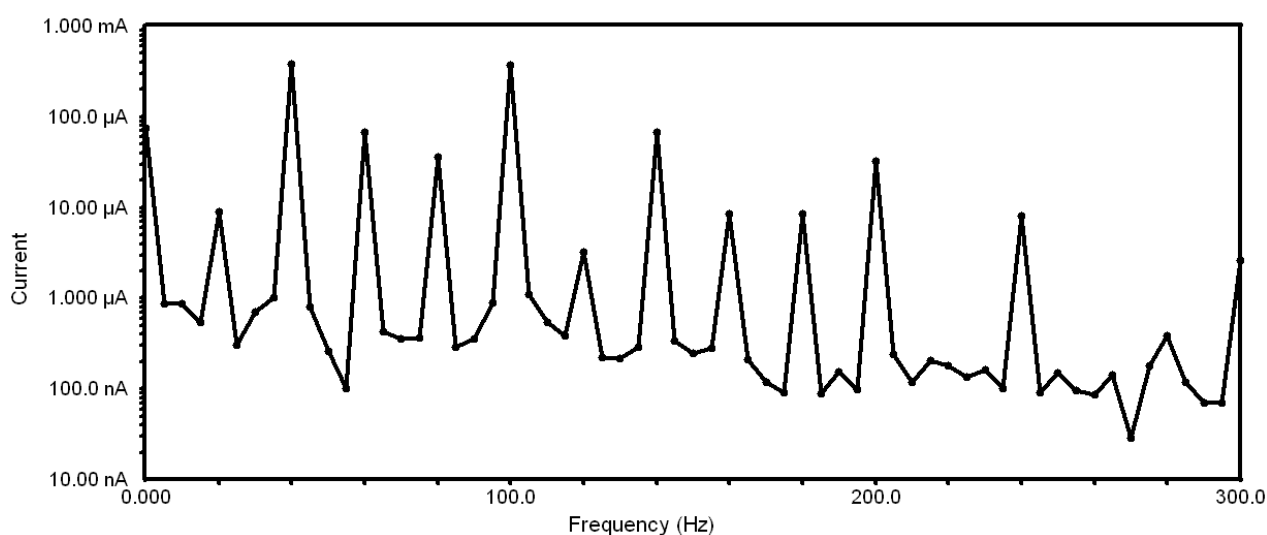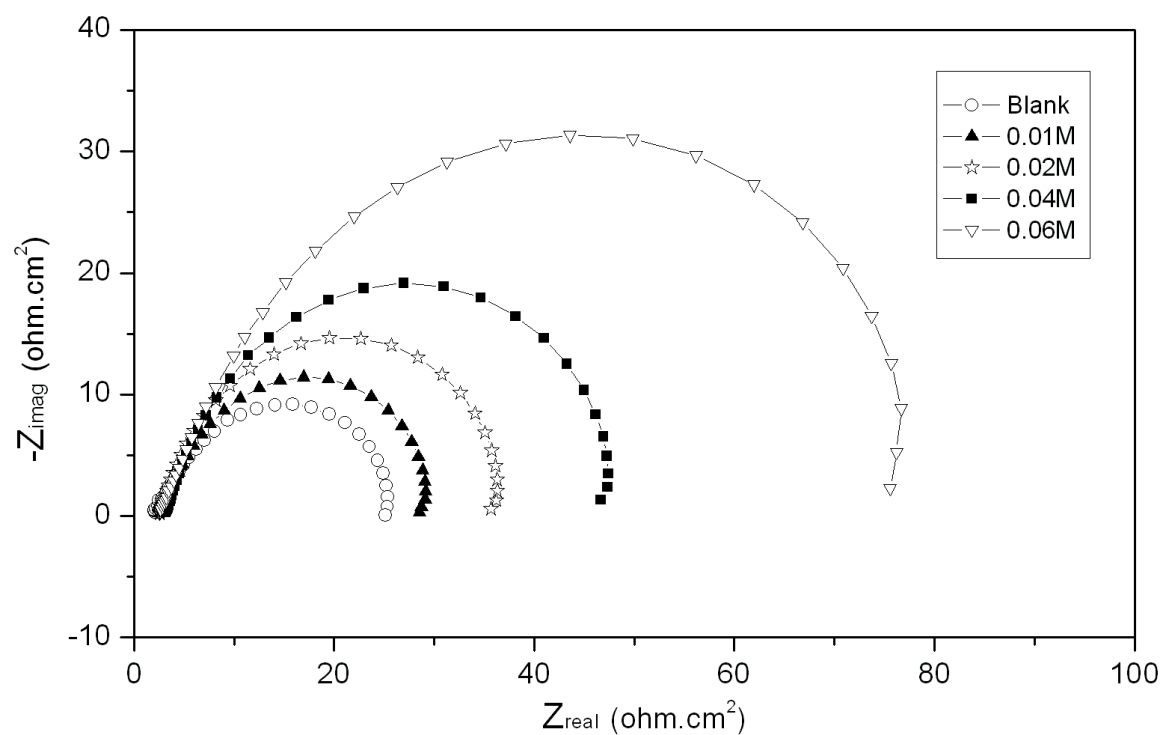
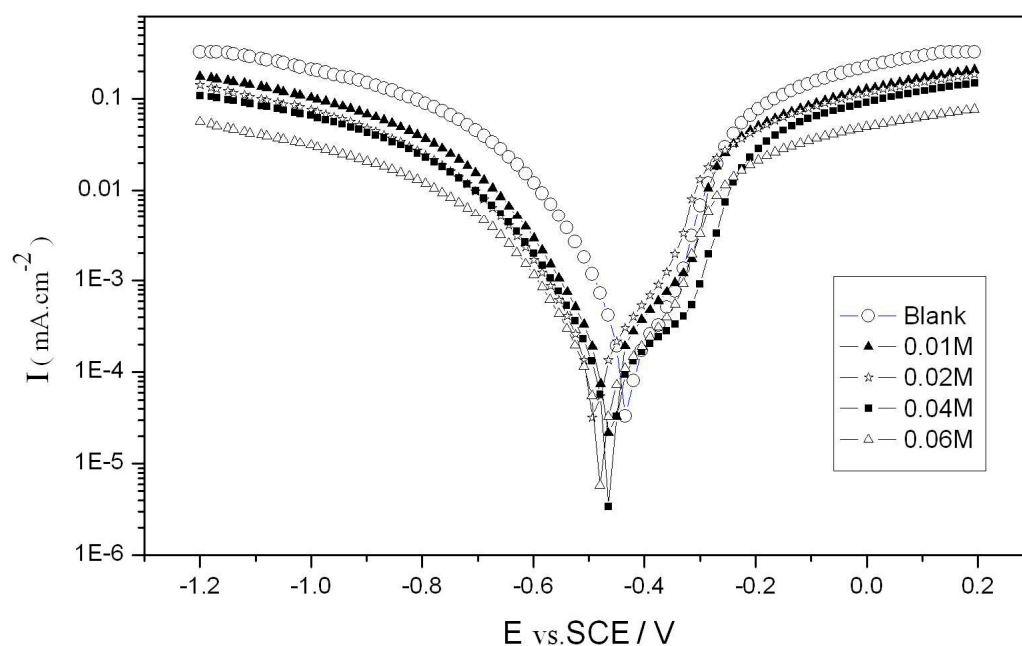## Figure (1a)
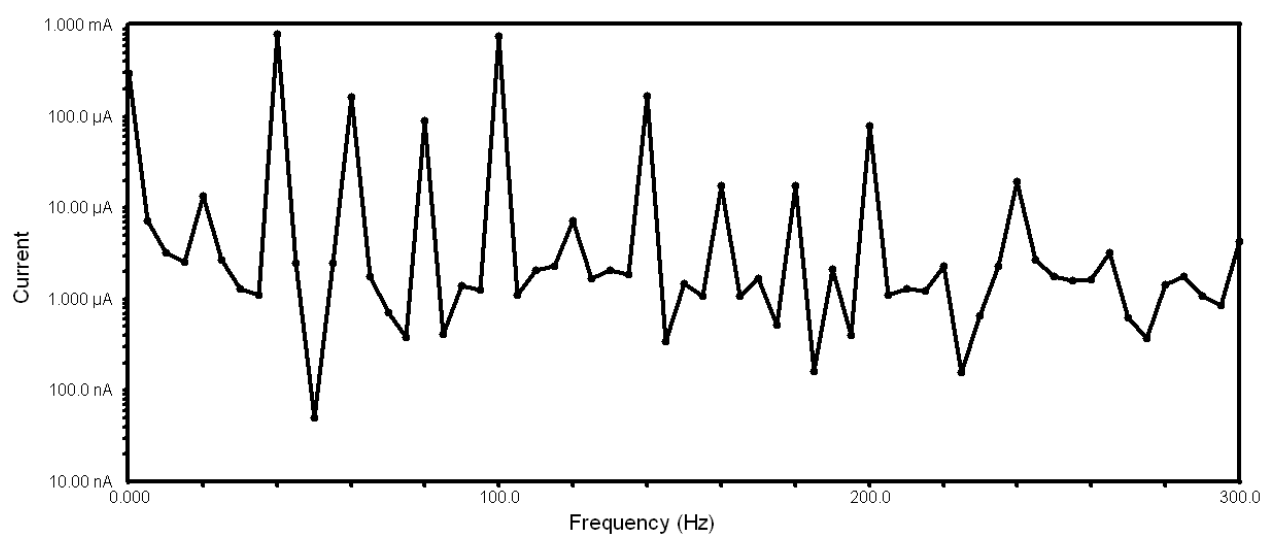
Figure (1b)

Figure (2)

Figure (3)

Figure (4)

Figure (5)

Figure (6)